False nonlinear effect in z-scan measurement based on semiconductor laser devices: theory and experiments

Hui Yan[1,2] and Jingsong Wei[1,*]

[1]*Shanghai Institute of Optics and Fine Mechanics, Chinese Academy of Sciences, Shanghai 201800, China*
[2]*University of Chinese Academy of Sciences, Beijing 100049, China*
**Corresponding author: weijingsong@siom.ac.cn*

Received December 3, 2013; revised January 23, 2014; accepted February 27, 2014;
posted February 27, 2014 (Doc. ID 202033); published March 26, 2014

With the development of semiconductor technology, semiconductor laser devices and semiconductor laser pump solid-state laser devices have been widely applied in z-scan experiments. However, the feedback light-induced output instability of semiconductor laser devices can negatively affect the accurate testing of the nonlinear index. In this work, the influence of feedback light on z-scan measurement is analyzed. Then the calculated formula of feedback light-induced false nonlinear z-scan curves is theoretically derived and experimentally verified. Two methods are proposed to reduce or eliminate the feedback light-induced false nonlinear effect. One is the addition of an attenuator to the z-scan optical path, and the other is the addition of an opto-isolator unit to the z-scan setup. The experimental and theoretical results indicate that the feedback light-induced false nonlinear effect is markedly reduced and can even be ignored if appropriate parameters are chosen. Thus, theoretical and experimental methods of eliminating the negative effect of feedback light on z-scan measurement are useful for accurately obtaining the nonlinear index of a sample.

OCIS codes: (190.0190) Nonlinear optics; (190.5970) Semiconductor nonlinear optics including MQW.
http://dx.doi.org/10.1364/PRJ.2.000051

1. INTRODUCTION

Optical nonlinear materials have been extensively applied in optical switching [1], optical limiting devices [2], optical lithography [3], optical data storage [4], and so on. Accurate determination of the optical nonlinear index is important in real applications. Many methods of measuring the nonlinear index have been developed [5]. Among them, the single-beam z-scan technique proposed by Sheik-Bahae *et al.* [6] is widely used because of its simplicity and high sensitivity. Various improvements have been proposed since the introduction of the z-scan method, including the time-resolved z-scan [7], phase object z-scan [8], beam radius measurement z-scan [9], reflection z-scan [10], single-shot reflection z-scan [11], and so on. Different beam profiles have also been tested, such as circularly symmetric [12], elliptic Gaussian [13], Gaussian–Bessel [14], flat-topped [15], top-hat [16], and polarization beams [17]. In addition, the sensitivity and accuracy of measurements have been improved with various data processing and fitting methods [18–21]. In the basic z-scan measurement, a collimated laser beam focused through a lens is perpendicularly (normally) incident on the sample surface, and the sample is scanned along the z axis (optical axis) through the focal point. If significant nonlinearity is observed in the sample, the light intensity at different z-scan positions either increases or decreases depending on the positive or negative sign of the nonlinear index. The recorded z-scan curves are compared with the theoretically determined fitting curves, and the index of the optical nonlinearity is subsequently extracted.

In z-scan measurement, laser pulses are repeatedly irradiated onto samples, and the light transmitted or reflected from the samples is constantly acquired until the measurement is completed. The laser device is one of the critical components of a z-scan system, and the stability of laser power is very important to accurately obtain the nonlinear index. Gas laser devices are generally more stable than solid-state laser devices and semiconductor laser diode (LD) devices; thus, gas laser devices are widely used in a z-scan setup. However, in recent years, the development of semiconductor technology has resulted in semiconductor laser devices and semiconductor laser pump solid-state laser devices being extensively applied in z-scan experiments because of their small size, compactness, long service life, low cost, and ability to be modulated and integrated [22].

In z-scan measurement, the optical beam needs to be normally incident on the sample surface, which causes the reflected light from the sample surface to go back to the resonant cavity of an LD. The output stability of an LD is very sensitive to feedback light, which may lead to the instability of the laser output [23,24] and to a negative effect on the accurate testing of the nonlinear index. In other words, laser pulses are inevitably reflected back to the LD, causing the instability of laser power that negatively influences the z-scan measurement. Feedback light from a sample surface, called external cavity feedback, is known to increase the reflectivity of the internal cavity surface of an LD [25–27]. The external cavity feedback reduces the output coupling, which results in lower output power [28]. In z-scan measurement, feedback light markedly influences the results of nonlinear index measurement because the intensity changes as the sample moves along the z axis. In this work, we first theoretically analyze the factors influencing external cavity feedback. We then perform experimental methods of reducing and eliminating the influence of feedback light on z-scan measurements.

This paper is organized as follows. Section 2 discusses the influence of external cavity feedback light on LD devices. Section 3 presents the experimental methods and results for reducing and eliminating feedback light influence, and Section 4 provides the conclusion.

2. INFLUENCE OF FEEDBACK LIGHT ON SEMICONDUCTOR LD DEVICES

A. Internal Cavity Characteristics of LD

Inside an LD, the medium junction interface forms a Fabry–Perot (F-P) resonator with two cleavage planes, whose reflectivity are R_1 and R_2, respectively (Fig. 1, inner cavity box). P_1 is the laser power from cleavage plane R_1, and P_1' is the laser power reflected by the cleavage plane R_2. The F-P resonator can be considered as an internal cavity of an LD. The light reflected back and forth inside the internal cavity is amplified, resulting in laser output with power P_2.

In the internal cavity, the light energy loss includes free-carrier absorption loss α_{fc}, diffraction loss α_{diff}, and output end loss $\alpha_T = (1/2l)\ln[1/R_1R_2]$, where l is the length of the F-P resonator [29]. The total loss is represented as follows:

$$\alpha = \alpha_{\text{fc}} + \alpha_{\text{diff}} + \alpha_T = \alpha_0 + \frac{1}{2l}\ln\frac{1}{R_1R_2}, \tag{1}$$

where $\alpha_0 = \alpha_{\text{fc}} + \alpha_{\text{diff}}$. When the balance between the gain and loss is reached, the threshold gain g_{th} is equal to the threshold loss, which can be written as follows:

$$g_{\text{th}} = \alpha_0 + \frac{1}{2l}\ln\frac{1}{R_1R_2}. \tag{2}$$

The threshold current is proportional to the threshold gain $I_{\text{th}} = C'g_{\text{th}}$, and the output power P_2 of an LD can be written as follows:

$$P_2 = (1-R_2)\frac{C}{g_{\text{th}}}(I - I_{\text{th}}) = (1-R_2)\left(\frac{CI}{\alpha_0 + \frac{1}{2l}\ln\frac{1}{R_1R_2}} - C'\right), \tag{3}$$

where C and C' are constants only related with semiconductor LD, and I is the injected current. Equation (3) shows that the output power of the LD is positively proportional to the injected current I, and a laser output is achieved only when $I > I_{\text{th}}$.

B. Influence of External Feedback Light on the Output Characteristics of an LD

In real LD applications, external feedback light into an LD usually exists and inevitably influences the output stability of the LD. Figure 1 shows a schematic of influence of external feedback light on the LD output power, where the external feedback light path can be considered as an external cavity. In Fig. 1(a), R_3 is the reflectivity of the external cavity output mirror, and P_2 and P_2' are the laser powers irradiating on and reflected from the external cavity mirror R_3, respectively. The length of the internal cavity l is in submillimeter magnitude, whereas the external cavity length L is in decimeter magnitude; thus, l can be ignored compared with L. According to the Fresnel reflection, the following equations can be obtained [28]:

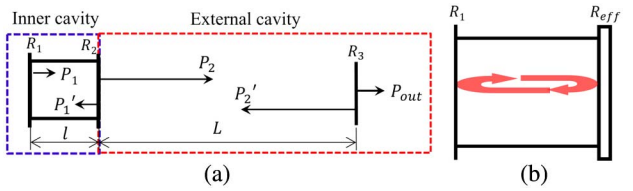

Fig. 1. Schematic of the far-field external cavity feedback influence on an LD: (a) detailed external feedback structure, (b) effective internal LD structure.

$$P_1' = R_2P_1 + (1-R_2)P_2', \tag{4}$$

$$P_2 = (1-R_2)P_1 + R_2P_2', \tag{5}$$

$$P_2' = R_3P_2. \tag{6}$$

To simplify the analysis, the internal and external cavities are combined into an effective internal LD structure, as presented in Fig. 1(b), where the effective reflectivity R_{eff} of the output plane of the internal LD structure can be written as

$$R_{\text{eff}} = \frac{P_1'}{P_1} = \frac{R_2 + R_3 - 2R_2R_3}{1 - R_2R_3}. \tag{7}$$

Figure 2(a) shows the dependence of R_{eff} on R_2 and R_3. When R_2 is close to unity, R_{eff} basically remains unchanged with R_3; however, when R_2 is much smaller than unity, R_3 has substantial influence on R_{eff}, and a larger R_3 results in a faster growth rate of R_{eff}.

Replacing R_2 in Eq. (2) with R_{eff} yields the threshold gain g_{th} of the effective internal LD structure:

$$g_{\text{th}} = \alpha_0 + \ln\frac{1}{R_1}\frac{1-R_2R_3}{R_2 + R_3 - 2R_2R_3}. \tag{8}$$

Equation (8) shows that the threshold gain g_{th} is determined by R_2 and R_3. R_2 is fixed for a given LD, whereas R_3 is the reflectivity of the external cavity. Thus, the external cavity characteristics significantly affects the threshold gain g_{th}. Substituting Eq. (8) into Eq. (3) yields the influence of the external cavity feedback light on the laser output of LD:

$$P_2 = (1-R_2)\left(\frac{CI}{\alpha_0 + \ln\frac{1}{R_1}\frac{1-R_2R_3}{R_2+R_3-2R_2R_3}} - C'\right). \tag{9}$$

Figure 2(b) shows the dependence of the output power P_2 on the reflectivity R_3 of the external cavity output mirror according to Eq. (9). To obtain a stable LD output, R_3 must be decreased as much as possible in the experiment.

C. Dynamic Characteristics of External Feedback in z-Scan Measurement

1. Analysis Based on Geometrical Optics

In z-scan measurement, the incident light from the LD is irradiated onto the sample after passing through a converging lens. The sample moves near the focal plane of the lens from the $-z$ direction to the $+z$ direction along the optical axis, where $-z$ and $+z$ indicate that the sample is on the left and right sides of the focal plane, respectively. When the

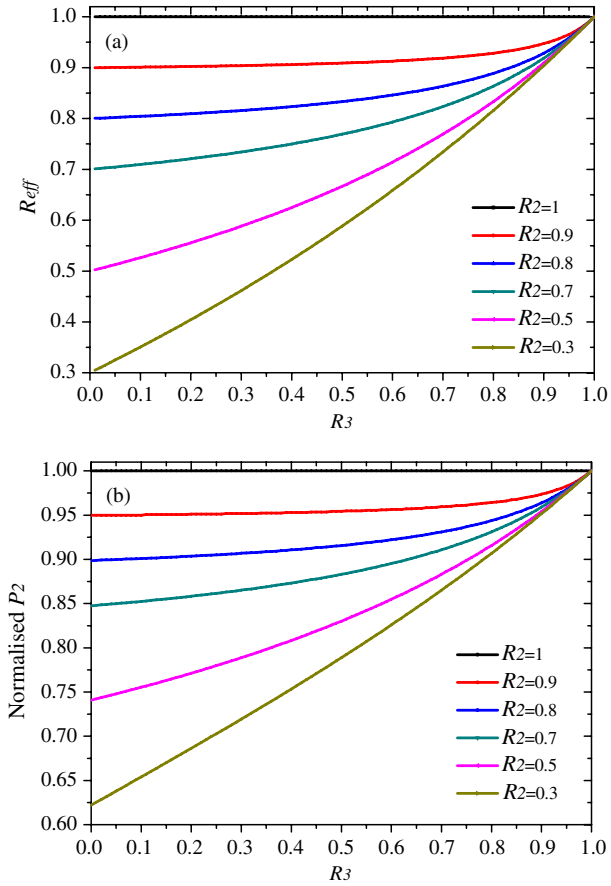

Fig. 2. Relationship among P_2, R_{eff}, and R_3 at different R_2 values: (a) dependence of R_{eff} on R_3, (b) dependence of P_2 on R_3.

sample moves along the optical axis, the nonlinearity of the sample changes the light propagation. Thus, the power detected by the detector varies with the sample position z, and the nonlinear index can be calculated accordingly. However, during measurement, some part of the incident light is reflected back to the LD by the sample, making the LD unstable. The intensity of reflected light into the LD changes with sample position z.

Figure 3 shows the reflected light changing with the sample position z, where the propagation locus of the edge line of the laser beam is schematically presented while the sample moves along the z direction. w_0 is the aperture radius of the LD, b is the distance from the LD to the lens, f is the focal length of the lens, and z is the distance between the sample and focal plane of the lens. In z-scan measurement, if the sample is on the focal plane [Fig. 3(b)], reflected light from the sample is collected by the lens and passes through the LD aperture and then back to the LD. However, if the sample is on the left of the focal plane ($-z$ direction), only partly reflected light goes back to the LD because of the limited aperture size of the LD, as shown in Fig. 3(a). If the sample is situated on the right side of the focal plane ($+z$ direction), reflected light is focused before entering the LD, similar to Fig. 3(a); only part of the reflected light goes back to the LD, as shown in Fig. 3(c).

The theoretical analysis is described as follows. In the z-scan measurement, a collimated Gaussian laser beam is emitted from the LD, and the electric field intensity is written as follows:

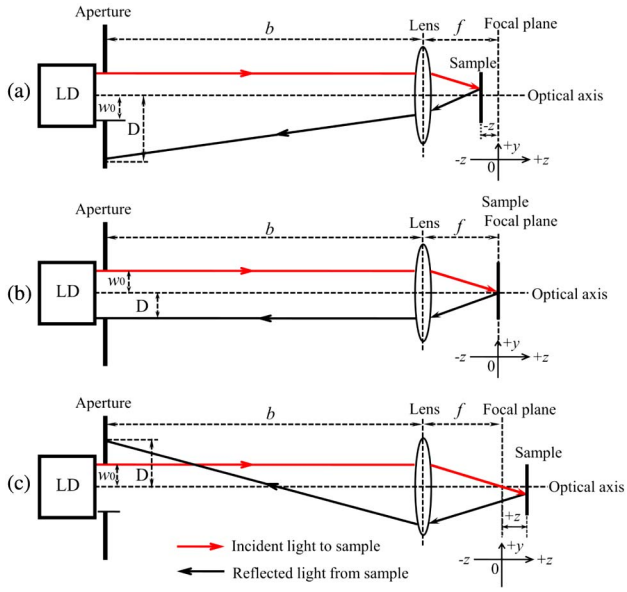

Fig. 3. Geometric simplification of laser beam propagation at different sample positions: (a) before the focal plane, (b) on the focal plane, (c) after the focal plane.

$$E(r) = E_0 \exp\left(-\frac{r^2}{w_0^2}\right), \tag{10}$$

where E_0 is the electric field amplitude and w_0 is the beam radius similar to the aperture radius of the LD. By a complex mathematical operation, the reflected beam radius in the LD plane can be written as follows:

$$D = \frac{2w_0}{f^2}|z|\left(b - \frac{f(f+2|z|)}{2|z|}\right). \tag{11}$$

Integrating laser intensity from the center to the aperture radius w_0, the laser power actually reflected back to the LD P_{reflect} is represented as follows:

$$\begin{aligned} P_{\text{reflect}} &= 2\pi E_0^2 \frac{w_0^2}{D^2}\int_0^{w_0} \exp\left(-\frac{2r^2}{D^2}\right) r\mathrm{d}r \\ &= \frac{1}{2}\pi w_0^2 E_0^2\left[1 - \exp\left(-\frac{2w_0^2}{D^2}\right)\right]. \end{aligned} \tag{12}$$

Substituting Eq. (11) into Eq. (12) yields the following equation:

$$P_{\text{reflect}} = \frac{1}{2}\pi w_0^2 E_0^2\left\{1 - \exp\left(-\frac{2f^4}{[2bz - f(f+2z)]^2}\right)\right\}. \tag{13}$$

Equation (13) indicates that the power of light reflected back to the LD changes with the sample position z. The dependence of P_{reflect} on the sample position z can be achieved by taking $b = 500$ mm, $f = 12$ mm as an example. The blue dotted line in Fig. 4 presents the normalized power P_{reflect} of the light reflected to the LD. We find that P_{reflect} dramatically changes when the sample moves backward and forward near the focal plane.

According to Fig. 1, the sample in the z-scan can be considered as an external feedback mirror, and the reflectivity is R_3.

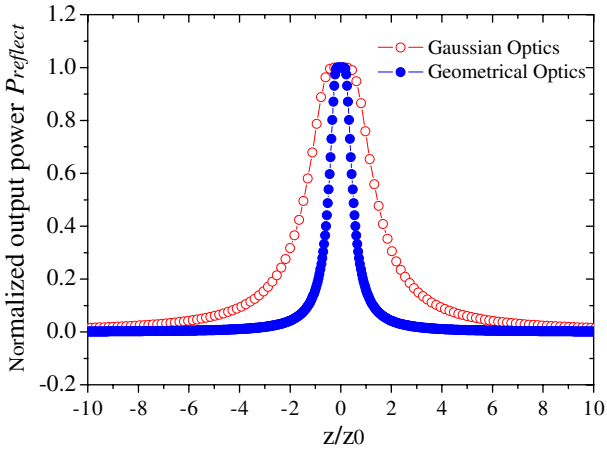

Fig. 4. Normalized reflected light power P_{reflect} using geometrical and Gaussian optics.

Thus, $P_{\text{reflect}} = R_3 P_{\text{in}}$, where $P_{\text{in}} = (1/2)\pi w_0^2 E_0^2$ is incident light power regardless of propagation energy loss. The following can be obtained from Eq. (13):

$$R_3 = 1 - \exp\left(-\frac{2f^4}{[2bz - f(f+2z)]^2}\right). \tag{14}$$

Equation (14) indicates that R_3 changes with the sample position z. Thus, according to Eq. (7), the effective reflectivity R_{eff} can be used to analyze the feedback light influence in the z-scan measurement.

2. Analysis Based on Gaussian Optics

The geometrical optics calculation is an intuitive method; here, in order to improve the calculation accuracy, the Gaussian optics calculation is also carried out. While a Gaussian distributed laser beam is travelling, the ABCD matrix is suitable for analyzing the propagation of the beam, which can simplify the calculation with a q factor. In the same system as Fig. 3, for a collimated incident laser beam, the q factor can be written as q_0:

$$q_0 = \mathrm{i}\frac{\pi w_0^2}{\lambda}. \tag{15}$$

By a series of mathematical operations, the ABCD propagation parameters are calculated as [30]:

$$\begin{bmatrix} A & B \\ C & D \end{bmatrix} = \begin{bmatrix} 1 & b \\ 0 & 1 \end{bmatrix}\begin{bmatrix} 1 & 0 \\ -\frac{1}{f} & 1 \end{bmatrix}\begin{bmatrix} 1 & 2f+2z \\ 0 & 1 \end{bmatrix}\begin{bmatrix} 1 & 0 \\ -\frac{1}{f} & 1 \end{bmatrix}\begin{bmatrix} 1 & b \\ 0 & 1 \end{bmatrix}$$
$$= \begin{bmatrix} \frac{2bz}{f^2} - \frac{2z}{f} - 1 & \frac{2b^2 z}{f^2} - \frac{4bz}{f} - 2f + 2z - 2b \\ \frac{2z}{f^2} & \frac{2bz}{f^2} - \frac{2z}{f} - 1 \end{bmatrix}. \tag{16}$$

The q factor of feedback light (marked as q_f) just before the LD is

$$q_f = \frac{Aq_0 + B}{Cq_0 + D}. \tag{17}$$

The laser radius D' just before the LD can be calculated as

$$D' = w'\sqrt{1 + \left(\frac{l}{z_r}\right)^2}. \tag{18}$$

The Rayleigh length z_r, the laser beam waist w', and the length l from the beam waist to the LD can be calculated with the imaginary and real parts of q_f, respectively:

$$z_r = \mathrm{Im}(q_f), \qquad w' = \sqrt{\frac{\lambda\,\mathrm{Im}(q_f)}{\pi}}, \qquad l = \mathrm{Re}(q_f). \tag{19}$$

Taking D' in place of D in Eq. (12) yields the reflected laser intensity P'_{reflect}:

$$P'_{\text{reflect}} = \frac{1}{2}\pi w_0^2 E_0^2\left[1 - \exp\left(-\frac{2\pi w_0^2}{\lambda\,\mathrm{Im}(q_f)\left(1 + \frac{\mathrm{Re}(q_f)^2}{\mathrm{Im}(q_f)^2}\right)}\right)\right]. \tag{20}$$

Normalized P'_{reflect} is shown in Fig. 4 (the red circled line). One can see from Fig. 4 that the basic trend of the geometrical optics calculation is basically consistent with that of the Gaussian optics calculation, and both of them show that the influence of feedback light depends on the sample location, especially near the focus of the lens. It needs to be pointed out that there are some small differences between the Gaussian optics and geometrical optics, which is because the accuracy of Gaussian optics calculation is better than geometrical optics. Compared with Gaussian optics analysis, the geometrical optics calculation is more intuitive and easy to understand.

D. Feedback Influence on the LD Output in z-Scan Measurement

In z-scan measurement, the incident light is reflected back to the LD by the sample, and the reflected light intensity is a function of the sample position z, which causes the instability of LD and induces a pseudo-nonlinearity effect. To monitor the instability of the LD and detect the pseudo-nonlinearity effect, three detectors in the optical path are placed in the traditional z-scan setup (Fig. 5). Detector 1 is used to collect feedback light from the sample, Detector 2 is placed in front of the lens to detect noise, and Detector 3 collects transmitted light through the sample.

In our experiment, the LD laser beam with a wavelength of 658 nm is used as a light source in the z-scan setup, and a BK7 glass about 1 mm thick is used as the sample. BK7 glass has no nonlinearity at low power irradiation; however, in our open-aperture z-scan experiment, the reflected light R_3 from BK7 glass presents a false nonlinear saturated absorption effect. It indicates that the instability of the LD is closely related to the external cavity reflectivity R_3, and feedback light from the sample causes LD to become unstable. A larger external

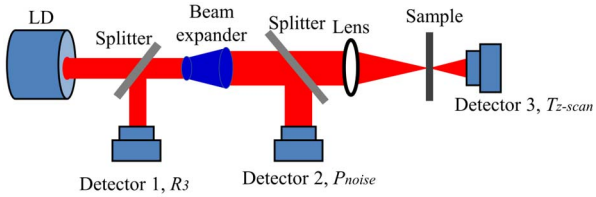

Fig. 5. Scheme of the z-scan equipment and its improvement.

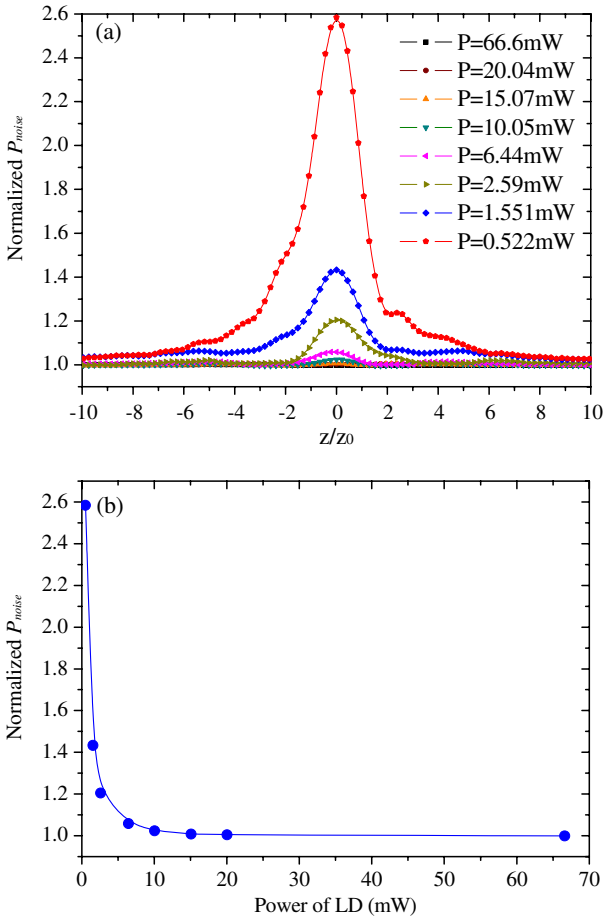

Fig. 6. Relationship among LD output power, P_{noise}, and sample position z: (a) normalized P_{noise} in z scan, (b) dependence of P_{noise} on LD power.

cavity reflectivity R_3 results in a larger reflectivity R_{eff} and greater LD instability.

Figure 6(a) shows the change in P_{noise} with the sample position z at different LD output powers. A lower LD output power corresponds to greater feedback light intensity. P_{noise} even reaches 260% when the LD power is 0.522 mW. Furthermore, the dependence of P_{noise} on the laser power of the LD is plotted, as shown in Fig. 6(b). P_{noise} exponentially decreases with increased LD power; that is, the influence of feedback light on LD output instability can be ignored when the LD power exceeds a certain value, which is useful for eliminating the reflected light influence on the LD during z-scan measurement.

3. ELIMINATION OF FEEDBACK LIGHT INFLUENCE ON z-SCAN MEASUREMENT

Theoretical analysis and experimental data show that in z-scan measurement, feedback light from the sample markedly influences nonlinearity measurement, which can induce a pseudo-nonlinearity effect. Thus, some experimental methods should be used to decrease and eliminate feedback light influence on z-scan measurement.

A. Decreasing Feedback Light Influence by Adding an Attenuator to the z-Scan Setup

Figure 6(b) indicates that the influence of feedback light on LD output instability can be reduced and ignored when the

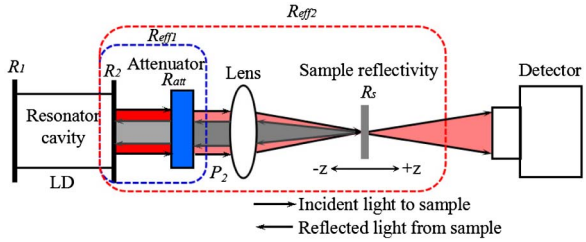

Fig. 7. Detailed illustration of the effective LD output with an attenuator.

LD power exceeds a certain value. Thus, in the z-scan setup, an attenuator can be placed after the LD, as shown in the blue box in Fig. 7. It shows a detailed illustration, where R_1 and R_2 are the reflectivities of cleavage plane 1 and cleavage plane 2, respectively, and R_{att} and R_s are the reflectivities of the attenuator and sample, respectively. The attenuator is a critical element for decreasing feedback light because of its distinctive advantages. Suppose the reflectivity of an attenuator is $R_{att} = 0.9$ and the reflectivity of the sample is $R_s = 0.3$. If the nonlinearity excitation power on the sample surface is required to be P, then the LD output should be set as P, regardless of energy loss without an attenuator, and the feedback light to LD is $0.3P$; that is, about 30% of the light energy is feedback to the LD. On the contrary, with the presence of an attenuator, the LD output power should be set as $10P$ because $R_{att} = 0.9$. Thus, the transmittance $T_{att} = 0.1$ and the feedback light to the LD should be $0.03P$; that is, only about 0.3% of the light energy is feedback to the LD. By contrast, the attenuator can reduce the feedback light to only 1% than that without an attenuator. Moreover, a larger LD output power leads to less influence on the LD from feedback light, as shown in Fig. 6(b). Thus, placing an attenuator in the z-scan setup can decrease the negative influence from feedback light during nonlinear measurement.

Figure 7 shows that the LD and attenuator can be considered as a new F-P resonator with effective cavity end reflectivity R_{eff1}, as shown in the blue dashed box. According to Eq. (7), the effective cavity end reflectivity can be written as follows:

$$R_{eff1} = \frac{R_2 + R_{att} - 2R_2R_{att}}{1 - R_2R_{att}}. \tag{21}$$

According to Fig. 1, considering R_s of sample surface reflectivity, the new F-P resonator and sample make up a new effective internal LD structure with reflectivity R_{eff2}, as shown in the red dashed box in Fig. 7. Replacing R_2, and R_3 by R_{eff1} and R_s in Eq. (7), respectively, the end reflectivity of the new effective internal LD structure is obtained as follows:

$$R_{eff2} = \frac{R_2 + R_{att} + R_s - 2R_2R_{att} - 2R_2R_s - 2R_{att}R_s + 3R_2R_{att}R_s}{1 - R_2R_{att} - R_2R_s - R_{att}R_s + 2R_2R_{att}R_s}. \tag{22}$$

Figure 8(a) presents the dependence of R_{eff2} on the sample reflectivity R_s at $R_2 = 0.3$. For a fixed R_2, a larger R_{att} leads to more stable R_{eff2}; that is, the stability of the LD can be improved by placing an attenuator after the LD. If $R_{att} = 0.9$, R_{eff2} is almost unchanged at $R_s < 0.5$, which is easily met in the z-scan because the sample is generally transparent

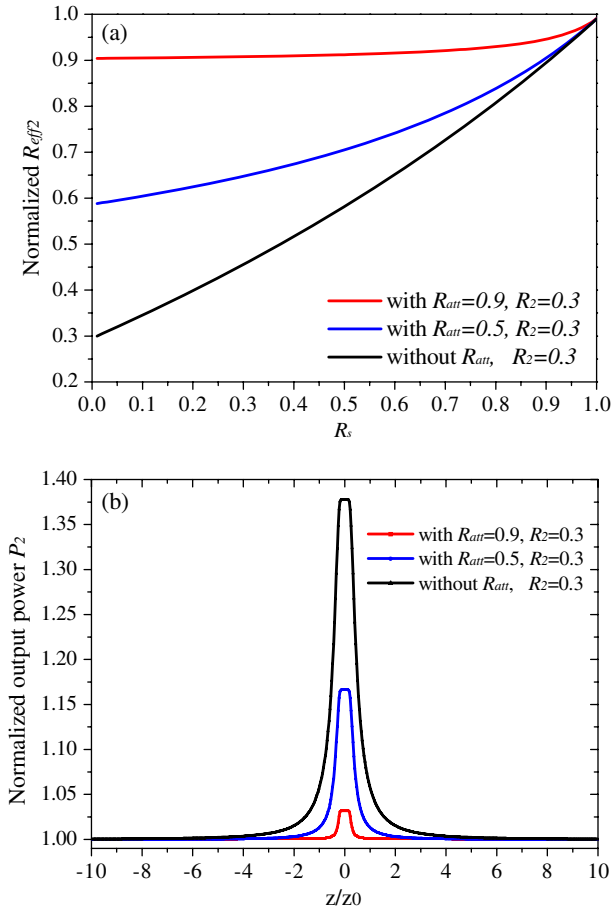

Fig. 8. Relationship of R_{eff2} and P_2 with different attenuations in z scan when $R_2 = 0.3$: (a) dependence of R_{eff2} on R_3, (b) dependence of P_2 on the z position.

or semitransparent. This result indicates that the external feedback influence caused by sample movement can be markedly reduced or even ignored.

According to Eq. (9), the output power P_2 of the new effective internal LD structure can be written as follows:

$$P_2 = (1 - R_{\text{eff1}})\left(\frac{CI}{\alpha_0 + \frac{1}{2l}\ln\frac{1}{R_1 R_{\text{eff2}}}} - C'\right). \tag{23}$$

Substituting Eqs. (15) and (16) into Eq. (17) yields the relationship of P_2 with the sample position z, as shown in Fig. 8(b). A larger R_{att} results in a more stable LD output power P_2. Compared with that without an attenuator ($R_{\text{att}} = 0$), the instability of the LD output P_2 is reduced to 0.83%; that is, the stability of the LD output is greatly improved in the z-scan measurement.

Figure 9 shows the open-aperture z-scan measurement results with a BK7 glass sample for different R_{att} values using the setup in Fig. 7, where the LD output power is set at $P = 1$ mW. The black dotted line shows that the interface reflectance from the glass sample exerts a strong false nonlinear saturated absorption effect without an attenuator on the optical path. A comparison among the curves in Fig. 9 indicates that the attenuator can obviously decrease the false nonlinear saturated absorption effect, which then decreases as the reflectivity of the attenuator R_{att} increases. The false nonlinear saturated absorption effect is almost eliminated at $R_{\text{att}} = 99.5\%$.

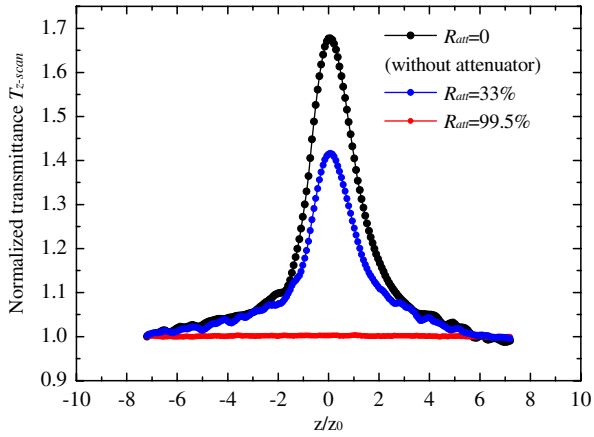

Fig. 9. Comparison of feedback influence with different attenuation values.

B. Decreasing Feedback Light Influence by Adding an Opto-isolator Unit to the z-Scan Setup

Another method is provided for decreasing and eliminating the influence of feedback light. An opto-isolator unit consisting of a half-wave plate, a polarized beam splitter (PBS), and a quarter-wave plate is placed in the z-scan setup, as shown in Fig. 10(a). The laser beam passes through the half-wave plate and becomes p-polarization light, which travels through the PBS and quarter-wave plate and then becomes circular polarization light. This circular polarization light is then split into two beams: one is detected by the noise detector that monitors the instability of the LD, and the other is focused by the lens and irradiated onto the sample to induce a nonlinear effect. The sample moves through the focal plane of the lens from the $-z$ to $+z$ direction, and then the light transmitted through the sample is collected by Detector 3. Moreover, some parts of the circular polarization light reflected by the sample pass through the quarter-wave plate again and become s-polarization light. This s-polarization light is perpendicular to the incident p-polarization light and thus cannot pass through the PBS and become feedback to the LD. The opto-isolator unit realizes the isolation of reflected light from sample to LD, and the feedback light influence on the z-scan measurement is reduced or even eliminated, theoretically. Figure 10(b) shows typical open-aperture experimental results where BK7 glass is used as a sample at $P = 1.52$ mW. Here one can notice that the laser power is low; actually, there are lots of examples where the optical nonlinearities are stimulated for such low values of the incident power, such as PtOx and $Ge_2Sb_2Te_5$ [31,32]. When no opto-isolator unit is placed in the optical path, the z-scan measurement of BK7 glass presents a strong nonlinear saturated absorption effect, and the normalized peak of $T_{z\text{-scan}}$ is about 2.8. When an opto-isolator unit is added to the z-scan setup with a maximum transmittance of 87.97% in experiment, the normalized peak of $T_{z\text{-scan}}$ is reduced to about 1.45. Thus, the opto-isolator unit is very useful for decreasing the influence of feedback light on z-scan measurement.

Figure 10 also indicates that thoroughly eliminating the influence of feedback light on z-scan measurement is difficult

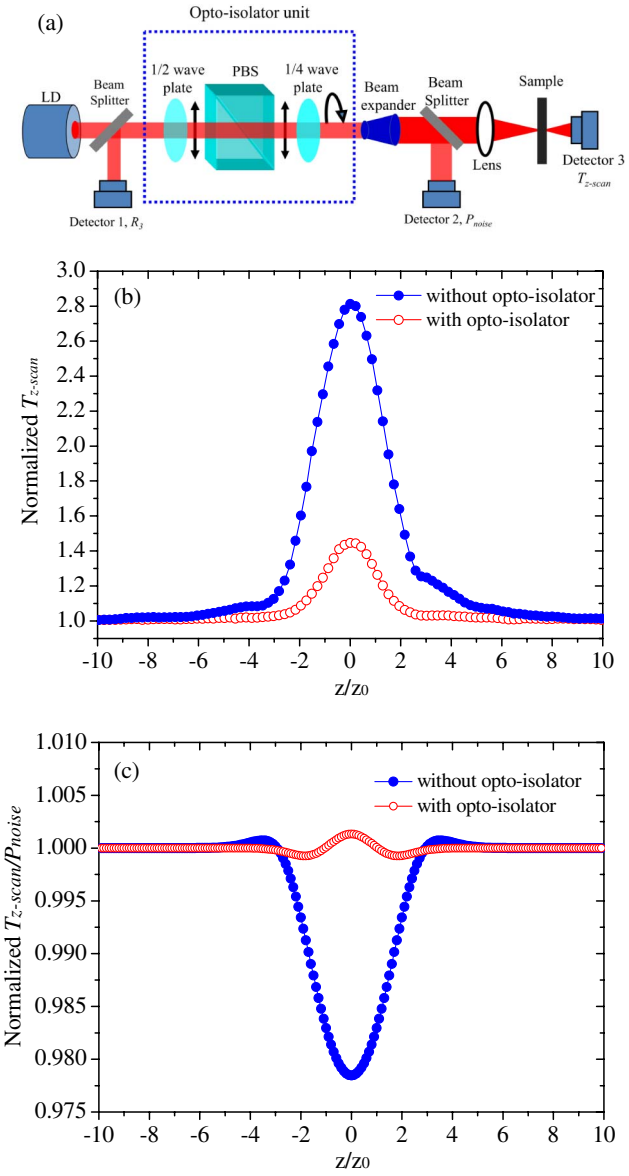

Fig. 10. Reduction of feedback light influence on open-aperture z-scan measurement: (a) z-scan experimental setup, (b) transmittance with and without an opto-isolator unit, (c) $T_{z\text{-scan}}/P_{\text{noise}}$ with and without an opto-isolator unit.

because a small leakage light inevitably feeds back to the LD and negatively affects the measurement accuracy. The noise detector, Detector 2, is thus inserted before the lens in the experimental setup in Fig. 10(a). Detector 2 is used to monitor and record the instability of the LD output P_{noise}, and the nonlinear measurement accuracy can be further improved by the numerical operation of $T_{z\text{-scan}}/P_{\text{noise}}$. Figure 10(c) shows the typical P_{noise} and $T_{z\text{-scan}}$ curves for BK7 glass sample under the conditions with and without the opto-isolator. The $T_{z\text{-scan}}$ peak value of 1.45 in the red circled line of Fig. 10(b) is reduced to a $T_{z\text{-scan}}/P_{\text{noise}}$ of 1.00133, which is much close to unity. Compared with the $T_{z\text{-scan}}/P_{\text{noise}}$ of 0.97846 without the opto-isolator, the maximum error influence is reduced from 2.154% without the opto-isolator to 0.133% with the opto-isolator.

Figures 11(a) and 11(b) give closed-aperture z-scan measurement results and $T_{z\text{-scan}}/P_{\text{noise}}$, respectively. One can find

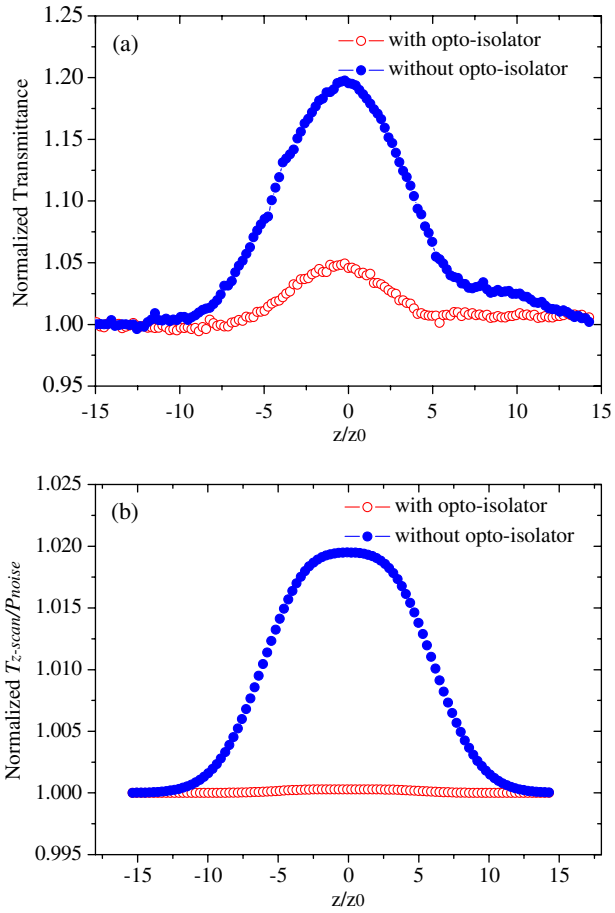

Fig. 11. Reduction of feedback light influence on closed-aperture z-scan measurement: (a) transmittance with and without an opto-isolator unit, (b) $T_{z\text{-scan}}/P_{\text{noise}}$ with and without an opto-isolator unit.

that opto-isolator is helpful in reducing the feedback light influence, and the transmittance peak value is reduced from 19.77% without the opto-isolator to 4.59% with the opto-isolator, and $T_{z\text{-scan}}/P_{\text{noise}}$ is reduced from 1.949% without the opto-isolator to 0.029% with the opto-isolator. Both improvements are significant because in many conditions the normalized transmittance variation is under 10% [6,33]. Besides, in a closed-aperture z-scan, there is only a peak instead of a peak–valley when there are nonlinear samples [6]. In other words, the z-scan measurement of the BK7 glass sample does not have a nonlinear effect. Therefore, both the optical isolator and the numerical calculation of $T_{z\text{-scan}}/P_{\text{noise}}$ can further decrease the influence of feedback light on the z-scan measurement. With these improvements, the false nonlinear effect induced by feedback light from the sample is almost eliminated.

4. SUMMARY

The output stability of an LD is very sensitive to the feedback light, which negatively affects the accurate testing of the nonlinear index in z-scan measurement. In this study, the influence of feedback light on z-scan measurement is analyzed. Then the calculation formulas of feedback light-induced false nonlinear z-scan curves are theoretically derived. Two methods are proposed to reduce or eliminate the feedback light-induced false nonlinear effect on z-scan measurement.

One is the addition of an attenuator to the z-scan optical path, and the other is the addition of an opto-isolator unit to the z-scan setup. The experimental results indicate that the feedback light-induced false nonlinear effect is markedly reduced by the improvements for the z-scan measurement setup. The feedback influence can even be eliminated if appropriate parameters are chosen.

ACKNOWLEDGMENTS

This work is partially supported by the National Natural Science Foundation of China (Nos. 51172253 and 61137002), the Instrument Developing Project of the Chinese Academy of Sciences (Grant No. YZ201140), and the Science and Technology Commission of Shanghai Municipality (11JC1412700 and 11JC1413300).

REFERENCES

1. J. Y. Lee, L. Yin, G. P. Agrawal, and P. M. Fauchet, "Ultrafast optical switching based on nonlinear polarization rotation in silicon waveguides," Opt. Express **18**, 11514–11523 (2010).
2. M. Sheik-Bahae, A. A. Said, D. J. Hagan, M. J. Soileau, and E. W. Van Stryland, "Nonlinear refraction and optical limiting in thick media," Opt. Eng. **30**, 1228–1235 (1991).
3. X. Ma and J. Wei, "Nanoscale lithography with visible light: optical nonlinear saturable absorption effect induced nanobump pattern structures," Nanoscale **3**, 1489–1492 (2011).
4. J. Wei, S. Liu, Y. Geng, Y. Wang, X. Li, Y. Wu, and A. Dun, "Nano-optical information storage induced by the nonlinear saturable absorption effect," Nanoscale **3**, 3233–3237 (2011).
5. J. Wei, ed., *Nonlinear Performance and Characterization Methods in Optics* (Nova Science, 2013).
6. M. Sheik-Bahae, A. A. Said, T. H. Wei, D. J. Hagan, and E. W. van Stryland, "Sensitive measurement of optical nonlinearities using a single beam," IEEE J. Quantum Electron. **26**, 760–769 (1990).
7. J. Wang, M. Sheik-Bahae, A. A. Said, D. J. Hagan, and E. W. van Stryland, "Time-resolved z-scan measurements of optical nonlinearities," J. Opt. Soc. Am. B **11**, 1009–1017 (1994).
8. J. Y. Yang, X. R. Zhang, Y. X. Wang, M. Shui, C. W. Li, X. Jin, and Y. L. Song, "Method with a phase object for measurement of optical nonlinearities," Opt. Lett. **34**, 2513–2515 (2009).
9. G. Tsigaridas, M. Fakis, I. Polyzos, P. Persephonis, and V. Giannetas, "Z-scan technique through beam radius measurements," Appl. Phys. B **76**, 83–86 (2003).
10. R. A. Ganeev and A. I. Ryasnyansky, "Reflection z-scan measurements of opaque semiconductor thin films," Phys. Status Solidi A **202**, 120–125 (2005).
11. R. A. Ganeev, "Single-shot reflection z-scan for measurements of the nonlinear refraction of nontransparent materials," Appl. Phys. B **91**, 273–277 (2008).
12. B. Rhee, J. S. Byun, and E. W. van Stryland, "Z-scan using circularly symmetric beams," J. Opt. Soc. Am. B **13**, 2720–2723 (1996).
13. G. Tsigaridas, M. Fakis, I. Polyzos, P. Persephonis, and V. Giannetas, "Z-scan technique for elliptic Gaussian beams," Appl. Phys. B **77**, 71–75 (2003).
14. S. Hughes and J. M. Burzler, "Theory of z-scan measurements using Ga'ussian–Bessel beams," Phys. Rev. A **56**, R1103–R1106 (1997).
15. J. Wang, B. Gu, Y. M. Xu, and H. T. Wang, "Enhanced sensitivity of z-scan technique by use of flat-topped beam," Appl. Phys. B **95**, 773–778 (2009).
16. W. Zhao and P. Palffy-Muhoray, "Z-scan technique using top-hat beams," Appl. Phys. Lett. **63**, 1613–1615 (1993).
17. X. Yan, Z. Liu, X. Zhang, W. Zhou, and J. Tian, "Polarization dependence of z-scan measurement: theory and experiment," Opt. Express **17**, 6397–6406 (2009).
18. G. Tsigaridas, M. Fakis, I. Polyzos, P. Persephonis, and V. Giannetas, "Z-scan analysis for high-order nonlinerities through Gaussian decomposition," Opt. Commun. **225**, 253–268 (2003).
19. E. Koushki, A. Farzaneh, and S. H. Mousavi, "Closed aperture z-scan technique using the Fresnel–Kirchhoff diffraction theory for materials with high nonlinear refractions," Appl. Phys. B **99**, 565–570 (2010).
20. F. Michelotti, F. Caiazza, G. Liakhou, S. Paoloni, and M. Bertolotti, "Effects of nonlinear Fabry-Pérot resonator response on z-scan measurements," Opt. Commun. **124**, 103–110 (1996).
21. E. Koushki and M. H. Majles Ara, "Comparison of the Gaussian-decomposition and the Fresnel-Kirchhoff diffraction methods in circular and elliptic Gaussian beams," Opt. Commun. **284**, 5488–5494 (2011).
22. B. Zhou, Y. Gao, C. Chen, and J. Chen, *The Principle of Laser* (National Defense Industry, 2009).
23. C. Masoller, A. C. Sicardi Schilino, and C. Cabeza, "Chaotic properties of the coherence collapsed state of laser diodes with optical feedback," Opt. Commun. **100**, 331–340 (1993).
24. R. Lang and K. Kobayashi, "External optical feedback effects on semi-conductor injection laser properties," IEEE J. Quantum Electron. **QE-16**, 347–355 (1980).
25. B. Tromborg, J. H. Osmundsen, and H. Olesen, "Stability analysis for a semiconductor laser in an external cavity," IEEE J. Quantum Electron. **QE-20**, 1023–1032 (1984).
26. C. Liu, J. Ge, and J. Chen, "Investigation of loss and threshold characteristics in the laser diode with external feedback," Chin. J. Lasers **31**, 1413–1416 (2004).
27. Y. Guo, Y. Wu, and Y. Wang, "Method to identify time delay of chaotic semiconductor laser with optical feedback," Chin. Opt. Lett. **10**, 061901 (2012).
28. C. Liu, J. Ge, and J. Chen, "Influence of external cavity feedback on the oscillating characteristics of a semiconductor laser," Acta Phys. Sin. **55**, 5211–5215 (2006).
29. B. Cai, Z. Liu, and X. Liu, "The structure, theory and characteristics of semiconductor lasers," in *Semiconductor Lasers* (Beijing Electronic Industry, 1995), pp. 40–42.
30. A. E. Siegmann, *Lasers* (University Science Books, 1986).
31. S. Liu, J. Wei, and F. Gan, "Optical nonlinear absorption characteristics of crystalline $Ge_2Sb_2Te_5$ thin films," J. Appl. Phys. **110**, 033503 (2011).
32. Y. H. Fu, Y. L. Lu, P. H. Chang, W. C. Hsu, S. Y. Tsai, and D. P. Tsai, "Z-scan study of nonlinear optical coupling of PtOx and $Ge_2Sb_2Te_5$ of near-field optical recording structure," Jpn. J. Appl. Phys **45**, 7224–7227 (2006).
33. L. Pálfalvi, B. C. Tóth, G. Almási, J. A. Fülöp, and J. Hebling, "A general Z-scan theory," Appl. Phys. B **97**, 679–685 (2009).